Electronic Supplementary Material (ESI) for New Journal of Chemistry.

SUPPLEMENTARY INFORMATION

Planar tetracoordinate carbon molecules with 14 valence electrons: the examples of $CBe_4M_n^{n-2}$ (M = Li, Au; *n* = 1–3) clusters

(Submitted to *New Journal of Chemistry*)

Jin-Chang Guo,[‡] Lin-Yan Feng,[‡] and Hua-Jin Zhai*

Nanocluster Laboratory, Institute of Molecular Science, Shanxi University, Taiyuan 030006, China

E-mail: hj.zhai@sxu.edu.cn

Table S1. Cartesian coordinates for global-minimum (GM) clusters **1**–**6** of the $CBe_4M_n^{n-2}$ (M = Li, Au; *n* = 1–3) series at the PBE0-D3/def2-TZVPP level, along with those for their three lowest-lying ***n*B**–***n*D** isomeric structures.

Table S2. Orbital composition analysis for the canonical molecular orbitals (CMOs) of GM CBe_4Li^- (**1**, C_{2v}, $^1A_1$) cluster. Main components greater than 15% are shown in bold.

Table S3. Orbital composition analysis for the CMOs of GM CBe_4Au^- (**4**, C_{2v}, $^1A_1$) cluster. Main components greater than 15% are shown in bold.

Table S4. Orbital composition analysis for the lowest unoccupied molecular orbitals (LUMOs) of the $CBe_4M_3^+$ (M = Li, Na, K, Cu, Ag, Au) series. Main components greater than 15% are shown in bold.

Figure S1. Optimized GM structures **1**–**6** of the $CBe_4M_n^{n-2}$ (M = Li, Au; n = 1–3) clusters at the PBE0-D3/def2-TZVPP level, along with their three lowest-lying isomers (***n*B**–***n*D**). Relative energies are listed in kcal mol^{-1} at the single-point CCSD(T) level using their PBE0-D3 geometries, with zero-point energy (ZPE) corrections at PBE0-D3. Shown in square brackets for comparison are the energetics at single-point CCSD(T)/def2-TZVPP//B3LYP-D3/def2-TZVPP level, including ZPE corrections at B3LYP-D3.

Figure S2. Calculated natural atomic charges (in |e|; red color) from natural bond orbital (NBO) analyses for GM clusters **1**–**6** of $CBe_4M_n^{n-2}$ (M = Li, Au; n = 1–3).

Figure S3. Calculated root-mean-square deviations (RMSDs) of GM clusters **1**–**6** of $CBe_4M_n^{n-2}$ (M = Li, Au; n = 1–3) during the Born-Oppenheimer molecular dynamics (BOMD) simulations at 298 K.

Figure S4. Pictures of the occupied CMOs of CBe_4Li^- (**1**) and CBe_4Au^- (**4**) clusters.

Figure S5. Optimized tetrahedral carbon (thC) isomeric structures **1′**/**3′**/**4′** at the PBE0-D3/def2-TZVPP level. These thC structures are to be compared to their GM ptC clusters **1**/**3**/**4**.

Figure S6. Comparison of Wiberg bond indices (WBIs) and natural atomic charges (in |e|; red color) of GM ptC cluster **3** and thC isomer **3′** at the PBE0-D3/def2-TZVPP level.

Figure S7. Nucleus independent chemical shifts (NICSs) for clusters **1**–**6**. Here the NICS(0) data (blue color) are calculated at the center of a triangle, whereas the NICS(1) values (red color) are at 1 Å above the center of a triangle or above the C center.

Table S1. Cartesian coordinates for global-minimum (GM) clusters **1**–**6** of the $CBe_4M_n^{n-2}$ (M = Li, Au; n = 1–3) series at the PBE0-D3/def2-TZVPP level, along with those for their three lowest-lying ***n*B**–***n*D** isomeric structures.

1 CBe_4Li^- (C_{2v}, $^1A_1$)				**1B** CBe_4Li^- (C_s, $^1A'$)			
C	0.00000000	0.70079500	0.00000000	C	−0.46275100	−0.36815500	0.00000000
Be	1.51006100	1.24431300	0.00000000	Be	−0.16507300	1.04326500	1.00147500
Be	−1.03601500	−0.66662900	0.00000000	Be	−0.16507300	−0.88359100	−1.49188900
Be	1.03601500	−0.66662900	0.00000000	Be	−0.16507300	−0.88359100	1.49188900
Be	−1.51006100	1.24431300	0.00000000	Be	−0.16507300	1.04326500	−1.00147500
Li	0.00000000	−2.94208000	0.00000000	Li	1.80589100	0.31051600	0.00000000
1C CBe_4Li^- (C_{2v}, $^1A_1$)				**1D** CBe_4Li^- (C_s, $^1A'$)			
C	0.00000000	0.28941800	0.00000000	C	0.00000000	0.56658900	0.00000000
Be	0.00000000	2.03918100	0.00000000	Be	−0.65976800	2.03264100	0.00000000
Be	0.00000000	−1.30417600	0.00000000	Be	−0.30452900	−1.13316900	0.00000000
Be	1.53583100	0.82307200	0.00000000	Be	1.45278600	−0.11018400	0.00000000
Be	−1.53583100	0.82307200	0.00000000	Be	−1.68942400	0.34858500	0.00000000
Li	0.00000000	−3.75370200	0.00000000	Li	1.60124600	−2.65034100	0.00000000
2 CBe_4Li_2 (C_s, $^1A'$)				**2B** CBe_4Li_2 (C_{2v}, $^1A_1$)			
C	0.00000000	−0.87197100	0.00000000	C	0.00000000	0.00000000	0.40514800
Be	−1.16713100	−1.97476900	0.00000000	Be	0.96738700	0.00000000	1.72502200
Be	0.31194300	0.82461900	0.00000000	Be	−0.96738700	0.00000000	1.72502200
Be	−1.50451600	−0.05143300	0.00000000	Be	0.00000000	1.34108800	−0.56976900
Be	1.58012100	−0.66292500	0.00000000	Be	0.00000000	−1.34108800	−0.56976900
Li	−1.52998700	2.47676900	0.00000000	Li	0.00000000	3.31541100	−1.94548500
Li	2.56943100	1.75318400	0.00000000	Li	0.00000000	−3.31541100	−1.94548500
2C CBe_4Li_2 (C_s, $^1A'$)				**2D** CBe_4Li_2 (C_s, $^1A'$)			
C	0.00000000	0.80696100	0.00000000	C	−0.43573800	−0.72017800	0.00000000
Be	−1.57373600	0.37070500	0.00000000	Be	−0.22350700	−1.18796500	1.52669400
Be	0.18461500	−0.92037900	0.00000000	Be	−0.22350700	−1.18796500	−1.52669400
Be	1.56820100	0.47790800	0.00000000	Be	−0.22350700	0.68498200	−1.02474800
Be	−1.70147100	−1.67369300	0.00000000	Be	−0.22350700	0.68498200	1.02474800
Li	2.35960600	−1.95106700	0.00000000	Li	1.78073500	−0.14423600	0.00000000
Li	−0.32975000	2.66442300	0.00000000	Li	0.28278100	2.92587900	0.00000000

3 $CBe_4Li_3^+$ (C_{2v}, $^1A_1$)			
C	0.00000000	0.79634400	0.00000000
Be	1.51832100	1.27286200	0.00000000
Be	−0.98723700	−0.59274800	0.00000000
Be	0.98723700	−0.59274800	0.00000000
Be	−1.51832100	1.27286200	0.00000000
Li	0.00000000	−2.96611500	0.00000000
Li	3.61781100	−0.22010500	0.00000000
Li	−3.61781100	−0.22010500	0.00000000

3B $CBe_4Li_3^+$ (C_s, $^1A'$)			
C	0.43999600	0.64025300	0.00000000
Be	1.51101700	−0.57281800	0.00000000
Be	−1.15313900	1.08558800	0.00000000
Be	−0.40504200	−0.96363200	0.00000000
Be	−2.39650500	−0.54204600	0.00000000
Li	0.79274400	1.57207600	1.71805700
Li	0.79274400	−3.10078000	0.00000000
Li	0.79274400	1.57207600	−1.71805700

3C $CBe_4Li_3^+$ (C_1, ^1A)			
C	0.46998900	−0.65524400	−0.14123000
Be	1.96818100	−0.52819500	−0.74533400
Be	−0.90889300	0.41009700	0.08814000
Be	−0.88742500	−1.52408800	−0.12918100
Be	0.93913400	1.04661000	−0.29724800
Li	1.56185100	−0.30406200	1.67968200
Li	−0.67374100	2.97124400	−0.01935000
Li	−3.30941900	−0.56259400	0.06695800

3D $CBe_4Li_3^+$ (C_s, $^1A'$)			
C	0.00000000	0.88823300	0.00000000
Be	0.89120100	−0.57982300	0.00000000
Be	1.55738200	1.22107400	0.00000000
Be	−0.49385300	−2.07860600	0.00000000
Be	−1.24487100	−0.14786000	0.00000000
Li	3.43455100	−0.56648300	0.00000000
Li	−1.08603800	2.47688300	0.00000000
Li	−3.29499200	−1.57324600	0.00000000

4 CBe_4Au^- (C_{2v}, $^1A_1$)			
C	0.00000000	−2.59567800	0.00000000
Be	1.49145000	−3.20436400	0.00000000
Be	−1.10820300	−1.29687800	0.00000000
Be	1.10820300	−1.29687800	0.00000000
Be	−1.49145000	−3.20436400	0.00000000
Au	0.00000000	0.65296200	0.00000000

4B CBe_4Au^- (C_{2v}, $^1A_1$)			
C	0.00000000	−2.85120200	0.00000000
Be	0.00000000	−4.59931500	0.00000000
Be	0.00000000	−1.27069500	0.00000000
Be	1.53682600	−3.38341200	0.00000000
Be	−1.53682600	−3.38341200	0.00000000
Au	0.00000000	0.85638700	0.00000000

4C CBe_4Au^- (C_s, $^1A'$)			
C	−0.27127300	−3.08091300	0.00000000
Be	1.25142500	−2.63036000	0.00000000
Be	−1.86978900	−3.15777600	0.00000000
Be	−0.72500200	−1.48706000	0.00000000
Be	1.75027500	−0.62703000	0.00000000
Au	0.00000000	0.63410600	0.00000000

4D CBe_4Au^- (C_s, $^1A'$)			
C	−0.45165600	−2.76050100	0.00000000
Be	1.07579700	−3.34396200	0.00000000
Be	0.81829800	−5.35136800	0.00000000
Be	−0.30252200	−1.18870800	0.00000000
Be	−0.91408900	−4.29701900	0.00000000
Au	0.00000000	0.92768700	0.00000000

5 CBe_4Au_2 (C_s, $^1A'$)				**5B** CBe_4Au_2 (C_{2v}, $^1A_1$)			
C	0.13822000	2.26366400	0.00000000	C	0.00000000	0.00000000	1.89112100
Be	1.63653200	1.75161000	0.00000000	Be	0.00000000	1.32714500	0.93518800
Be	0.00000000	0.58428600	0.00000000	Be	0.96892700	0.00000000	3.21868600
Be	−0.63271700	3.69218900	0.00000000	Be	−0.96892700	0.00000000	3.21868600
Be	−1.58194600	2.01497900	0.00000000	Be	0.00000000	−1.32714500	0.93518800
Au	−2.04533900	−0.18899100	0.00000000	Au	0.00000000	3.01255600	−0.28213800
Au	2.06411400	−0.39017600	0.00000000	Au	0.00000000	−3.01255600	−0.28213800
5C CBe_4Au_2 (C_s, $^1A'$)				**5D** CBe_4Au_2 (C_{2v}, $^1A_1$)			
C	1.19649400	−0.02446900	0.00000000	C	0.00000000	0.66590000	0.00000000
Be	0.36437700	−1.40058500	0.00000000	Be	1.46736300	1.23671300	0.00000000
Be	2.01179100	1.49361900	0.00000000	Be	0.95989800	−0.78326300	0.00000000
Be	0.00000000	1.00946900	0.00000000	Be	−1.46736300	1.23671300	0.00000000
Be	2.82579900	−0.23196500	0.00000000	Be	−0.95989800	−0.78326300	0.00000000
Au	0.36773500	3.14068600	0.00000000	Au	−3.19678300	−0.04824700	0.00000000
Au	−0.72199800	−3.18290500	0.00000000	Au	3.19678300	−0.04824700	0.00000000
6 $CBe_4Au_3^+$ (C_{2v}, $^1A_1$)				**6B** $CBe_4Au_3^+$ (C_{2v}, $^1A_1$)			
C	−0.00028200	−1.41621900	0.00000000	C	0.00000000	0.40165200	0.00000000
Be	−1.46274500	−2.04734700	0.00000000	Be	1.54528600	0.00139300	0.00000000
Be	−1.03784400	−0.07427800	0.00000000	Be	0.00000000	2.03683400	0.00000000
Be	1.46219000	−2.04755600	0.00000000	Be	0.00000000	−1.29949800	0.00000000
Be	1.03750800	−0.07477700	0.00000000	Be	−1.54528600	0.00139300	0.00000000
Au	3.20420400	−0.77585300	0.00000000	Au	−2.11962200	−2.08020100	0.00000000
Au	0.00047400	1.87376000	0.00000000	Au	0.00000000	4.09242200	0.00000000
Au	−3.20461100	−0.77546200	0.00000000	Au	2.11962200	−2.08020100	0.00000000
6C $CBe_4Au_3^+$ (C_{3v}, $^1A_1$)				**6D** $CBe_4Au_3^+$ (C_{2v}, $^1A_1$)			
C	0.00000000	0.00000000	2.31557300	C	0.00000000	0.00000000	0.35150900
Be	0.00000000	0.00000000	0.37585900	Be	0.00000000	1.31937300	−0.65767600
Be	1.32388000	−0.76434300	1.86646200	Be	0.00000000	−1.31937300	−0.65767600
Be	0.00000000	1.52868500	1.86646200	Be	−0.99876900	0.00000000	1.62635200
Be	−1.32388000	−0.76434300	1.86646200	Be	0.99876900	0.00000000	1.62635200
Au	0.00000000	2.24657900	−0.15947000	Au	0.00000000	0.00000000	3.59484400
Au	1.94559400	−1.12328900	−0.15947000	Au	0.00000000	−2.98160400	−1.85981700
Au	−1.94559400	−1.12328900	−0.15947000	Au	0.00000000	2.98160400	−1.85981700

Table S2. Orbital composition analysis for the canonical molecular orbitals (CMOs) of GM CBe_4Li^- (**1**, C_{2v}, $^1A_1$) cluster. Main components greater than 15% are shown in **bold**.

Subsystem	CMO	C (%)		Be_4 (%)		Li (%)	
		s/p	total	s/p	total	s/p	total
Be-Be 2c-2e σ	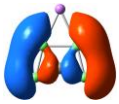 HOMO (b_2)	0.00/5.78	5.78	**44.76**/**45.44**	**90.20**	0.00/3.20	3.20
	 HOMO−1 (a_1)	2.72/4.03	6.75	**26.02**/**62.62**	**88.64**	3.80/0.18	3.98
Be-Li-Be 3c-2e σ	 HOMO−2 (a_1)	2.35/11.56	13.91	**55.16**/**18.26**	**73.42**	11.67/0.16	11.83
2π aromaticity	 HOMO−3 (b_1)	0.00/**70.04**	**70.04**	0.00/**29.14**	**29.14**	0.00/0.16	0.16
6σ aromaticity	 HOMO−4 (a_1)	2.47/**67.96**	**70.41**	12.70/14.54	**27.24**	1.36/0.28	1.64
	 HOMO−5 (b_2)	0.00/**79.30**	**79.30**	10.22/4.96	**15.18**	0.00/0.10	0.10
	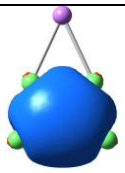 HOMO−6 (a_1)	**66.72**/0.98	**67.70**	**15.76**/**15.72**	**31.48**	0.10/0.06	0.16

Table S3. Orbital composition analysis for the CMOs of GM CBe_4Au^- (**4**, C_{2v}, $^1A_1$) cluster. Main components greater than 15% are shown in **bold**.

Subsystem	CMO	C (%)		Be_4 (%)		Au (%)	
		s/p	total	s/p	total	s,p/d	total
Be-Be 2c-2e σ	 HOMO (b_2)	0.00/5.50	5.50	**46.12**/**43.52**	**89.64**	2.50/1.48	3.98
	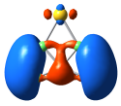 HOMO–1 (a_1)	5.29/0.56	5.85	**51.22**/**39.44**	**90.66**	2.50/0.58	3.08
Be-Au-Be 3c-2e σ	 HOMO–3 (a_1)	0.07/**42.52**	**42.59**	11.06/12.82	**23.88**	**31.14**/1.89	**33.13**
2π aromaticity	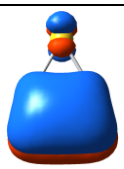 HOMO–2 (b_1)	0.00/**69.77**	**69.77**	0.00/**26.4**	**26.4**	0.25/3.04	3.29
6σ aromaticity	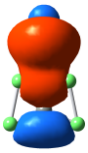 HOMO–4 (a_1)[a]	0.72/**22.98**	**23.70**	7.46/6.92	14.38	14.49/**47.41**	**61.90**
	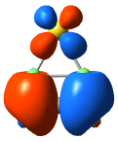 HOMO–9 (b_2)[b]	0.00/**67.93**	**67.93**	11.12/7.08	**18.20**	0.17/13.32	13.49
	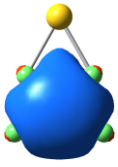 HOMO–11 (a_1)	**65.33**/1.04	**66.37**	**16.30**/**15.62**	**31.92**	0.53/0.47	1.00

(continued …)

Subsystem	CMO	C (%)		Be_4 (%)		Au (%)	
		s/p	total	s/p	total	s,p/d	total
Au lone pairs	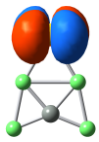 HOMO−5 (a_2)	0.00/0.00	0.00	0.00/0.56	0.56	0.00/**99.44**	**99.44**
	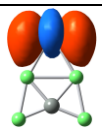 HOMO−6 (a_1)	0.00/0.00	0.00	1.54/1.44	2.98	1.75/**95.18**	**96.93**
	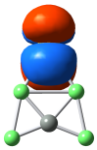 HOMO−7 (b_1)	0.00/1.37	1.37	0.00/2.52	2.52	0.00/**95.98**	**95.98**
	 HOMO−8 (b_2)	0.00/11.47	11.47	0.98/5.42	6.40	0.00/**81.98**	**81.98**
	 HOMO−10 (a_1)	2.65/**17.13**	**19.78**	5.60/12.88	**18.48**	9.16/**52.09**	**61.25**

[a] The destructive recombination between HOMO−4 and HOMO−10 recovers a true σ bond around the CBe_4 core; its constructive counterpart is a relatively pure Au d_z^2 lone-pair.

[b] Similar to the above, the destructive recombination between HOMO−9 and HOMO−8 recovers a true σ bond around the CBe_4 core; its constructive counterpart is a relatively pure Au d_{xz} lone-pair.

Table S4. Orbital composition analysis for the lowest unoccupied molecular orbitals (LUMOs) of the $CBe_4M_3^+$ (M = Li, Na, K, Cu, Ag, Au) series. Main components greater than 15% are shown in **bold**.

Species	LUMO	Symmetry	Be_4 (%)	M_3 (%)	C (%)
$CBe_4Li_3^+$	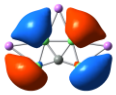	b_2	**88.01**	11.99	0.00
$CBe_4Na_3^+$	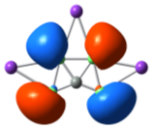	b_2	**93.16**	6.81	0.03
$CBe_4K_3^+$	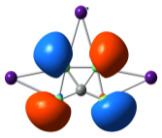	b_2	**92.10**	7.83	0.07
$CBe_4Cu_3^+$	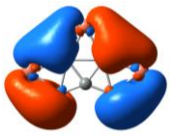	b_2	**87.24**	12.75	0.01
$CBe_4Ag_3^+$	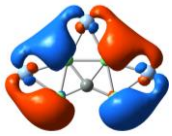	b_2	**89.22**	10.76	0.02
$CBe_4Au_3^+$	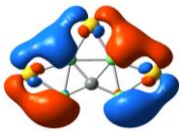	b_2	**85.5**	14.48	0.02

Figure S1. Optimized GM structures **1**–**6** of the $CBe_4M_n^{n-2}$ (M = Li, Au; n = 1–3) clusters at the PBE0-D3/def2-TZVPP level, along with their three lowest-lying isomers (***n*B**–***n*D**). Relative energies are listed in kcal mol^{-1} at the single-point CCSD(T) level using their PBE0-D3 geometries, with zero-point energy (ZPE) corrections at PBE0-D3. Shown in square brackets for comparison are the energetics at single-point CCSD(T)/def2-TZVPP//B3LYP-D3/def2-TZVPP level, including ZPE corrections at B3LYP-D3.

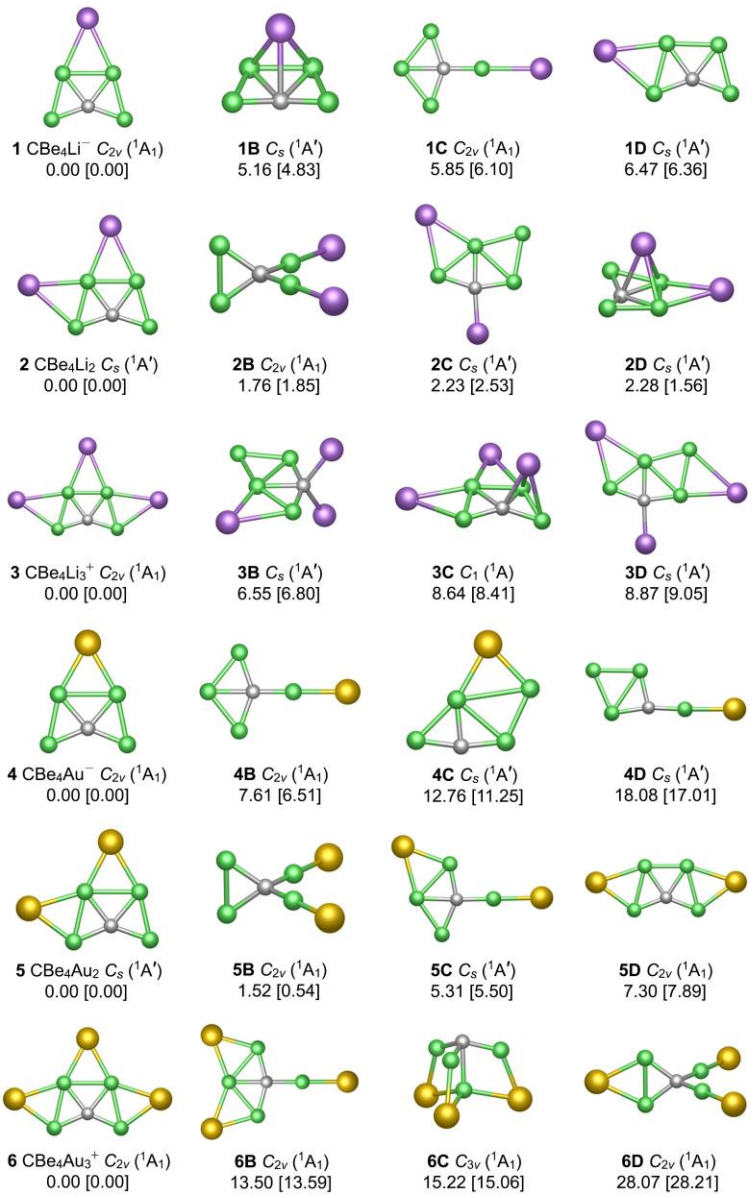

Figure S2. Calculated natural atomic charges (in |e|; red color) from natural bond orbital (NBO) analyses for GM clusters **1**–**6** of $CBe_4M_n^{n-2}$ (M = Li, Au; n = 1–3).

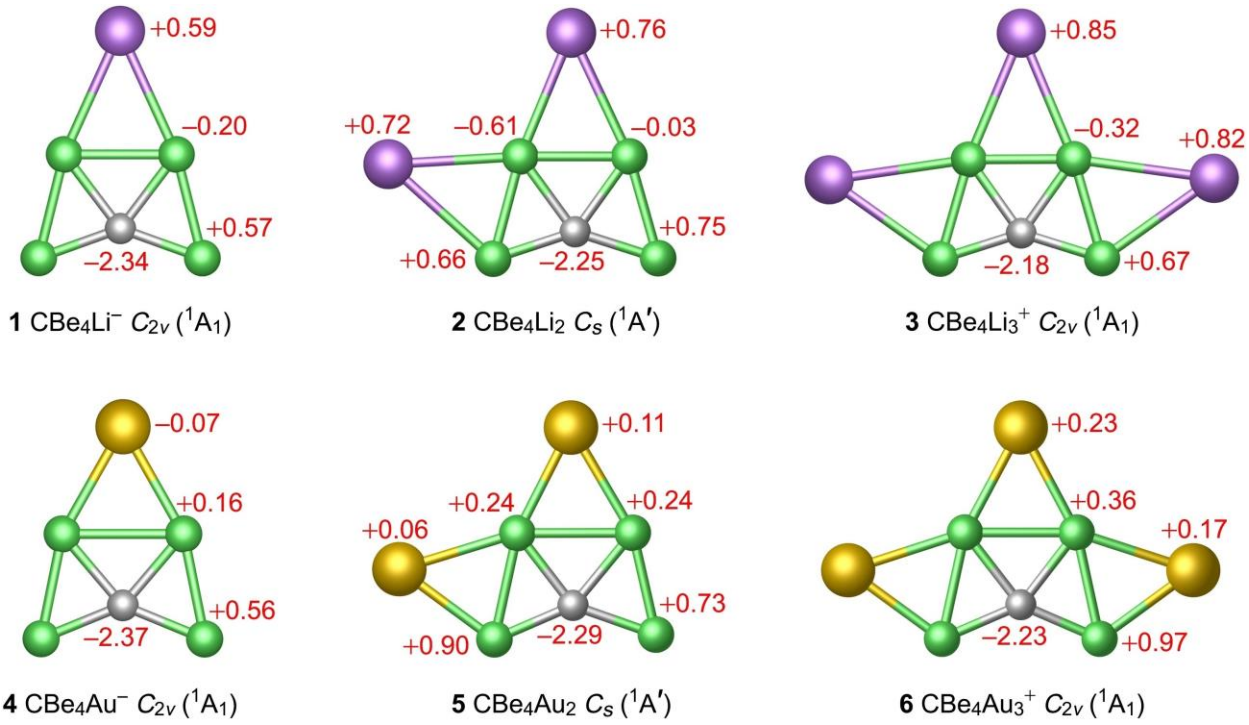

1 CBe_4Li^- C_{2v} ($^1A_1$) **2** CBe_4Li_2 C_s ($^1A'$) **3** $CBe_4Li_3^+$ C_{2v} ($^1A_1$)

4 CBe_4Au^- C_{2v} ($^1A_1$) **5** CBe_4Au_2 C_s ($^1A'$) **6** $CBe_4Au_3^+$ C_{2v} ($^1A_1$)

Figure S3. Calculated root-mean-square deviations (RMSDs) of GM clusters **1**–**6** of $CBe_4M_n^{n-2}$ (M = Li, Au; n = 1–3) during the Born-Oppenheimer molecular dynamics (BOMD) simulations at 298 K.

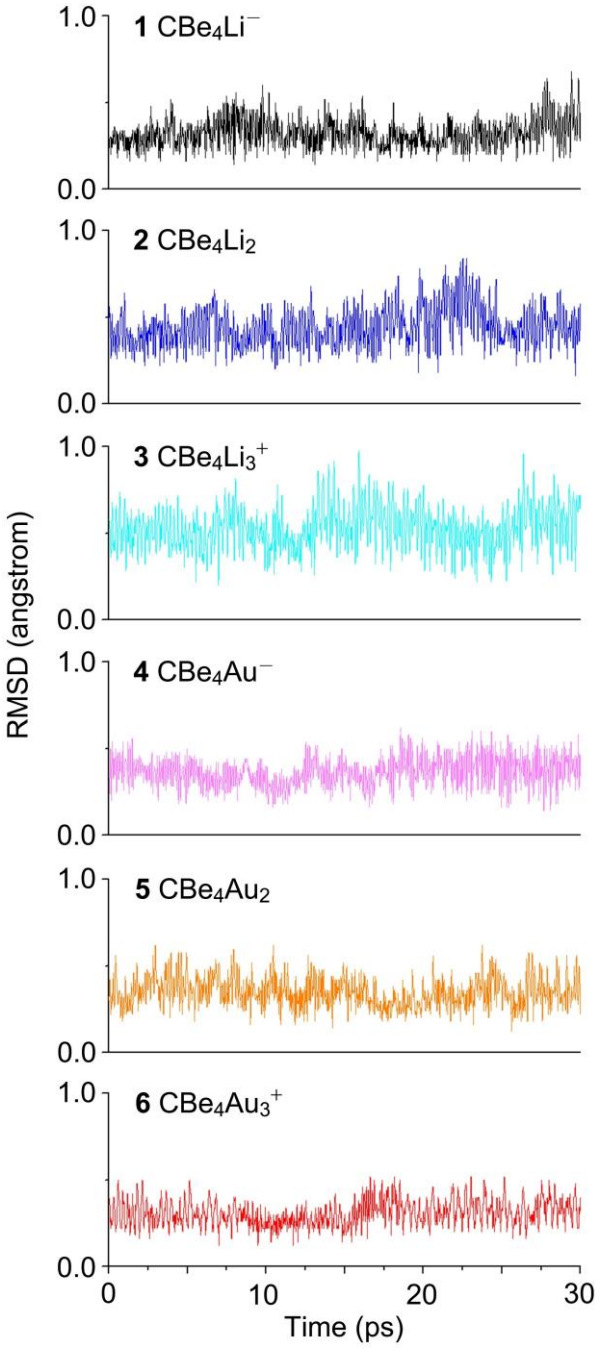

Figure S4. Pictures of the occupied CMOs of CBe_4Li^- (**1**) and CBe_4Au^- (**4**) clusters.

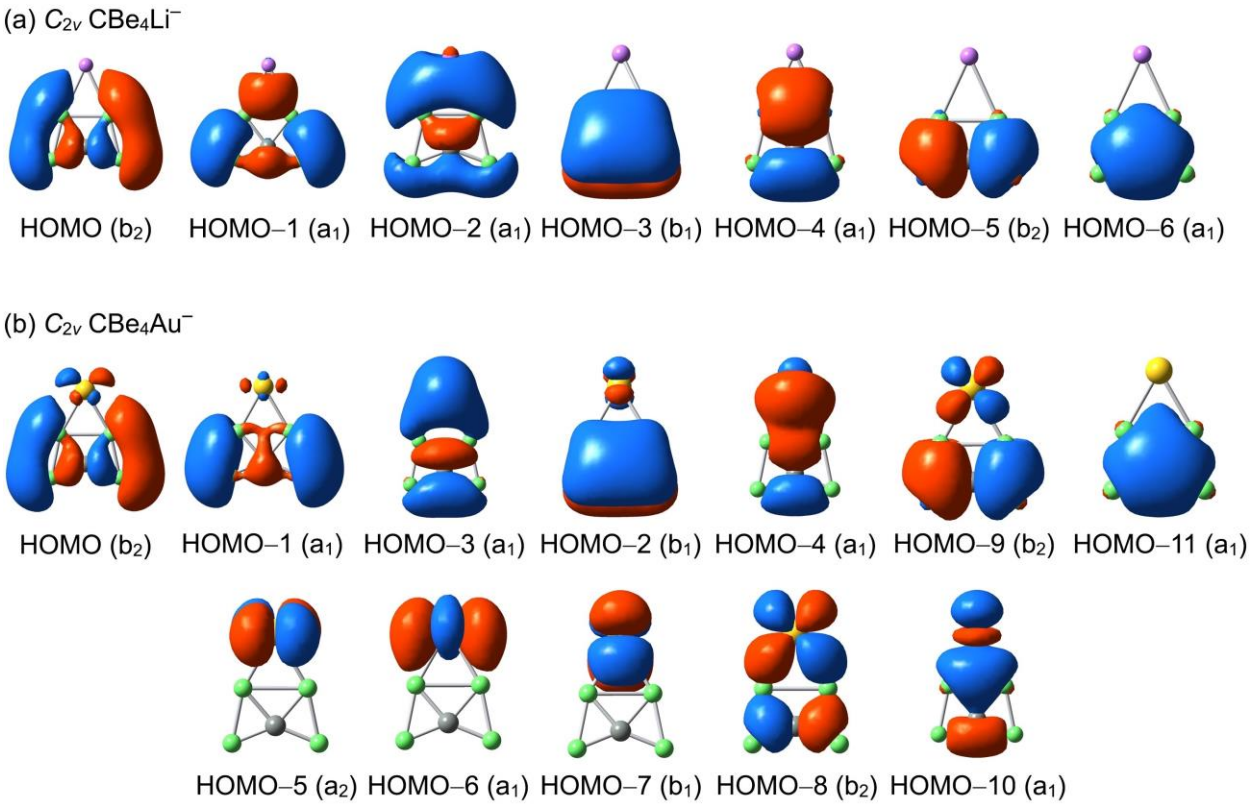

Figure S5. Optimized tetrahedral carbon (thC) isomeric structures **1′**/**3′**/**4′** at the PBE0-D3/def2-TZVPP level. These thC structures are to be compared to their GM ptC clusters **1**/**3**/**4**.

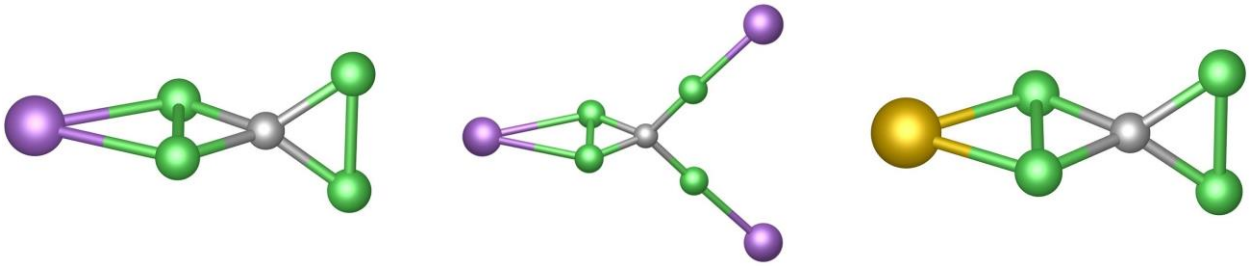

1′ CBe_4Li^- C_{2v} ($^1A_1$) **3′** $CBe_4Li_3^+$ C_{2v} ($^1A_1$) **4′** CBe_4Au^- C_{2v} ($^1A_1$)

Figure S6. Comparison of Wiberg bond indices (WBIs) and natural atomic charges (in |e|; red color) of GM ptC cluster **3** and thC isomer **3′** at the PBE0-D3/def2-TZVPP level.

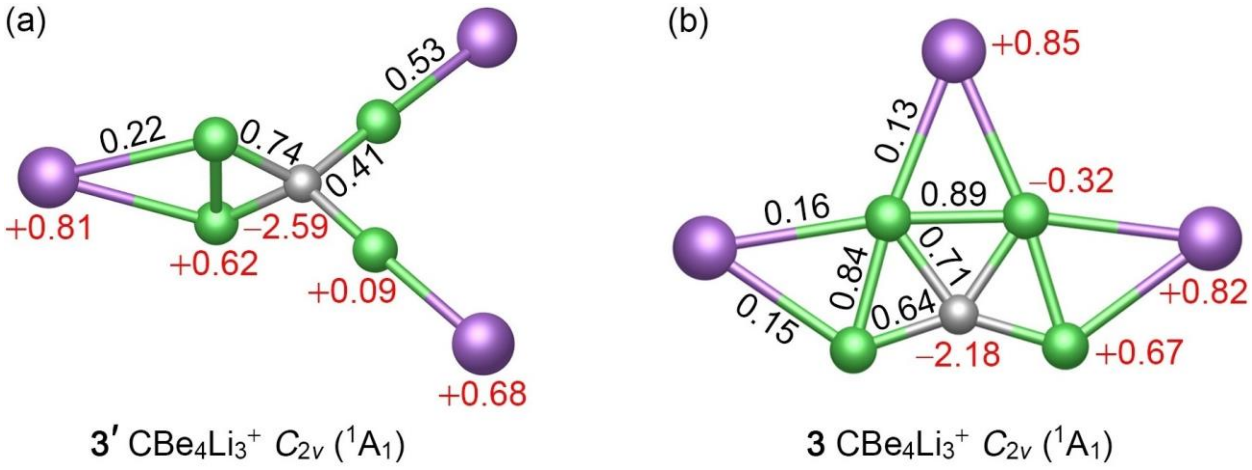

Figure S7. Nucleus independent chemical shifts (NICSs) for clusters **1**–**6**. Here the NICS(0) data (blue color) are calculated at the center of a triangle, whereas the NICS(1) values (red color) are at 1 Å above the center of a triangle or above the C center.